Cell Stem Cell
Article

Regulated Segregation of Kinase Dyrk1A during Asymmetric Neural Stem Cell Division Is Critical for EGFR-Mediated Biased Signaling

Sacri R. Ferron,[1,5] Natividad Pozo,[1,4] Ariadna Laguna,[2,4,6] Sergi Aranda,[2,4,7] Eva Porlan,[1] Mireia Moreno,[1] Cristina Fillat,[2] Susana de la Luna,[2,3] Pilar Sánchez,[1,8] María L. Arbonés,[2,*] and Isabel Fariñas[1,*]
[1]Departamento de Biología Celular and Centro de Investigación Biomédica en Red de Enfermedades Neurodegenerativas (CIBERNED), Universidad de Valencia, 46100 Burjassot, Spain
[2]Center for Genomic Regulation (CRG), UPF, and Centro de Investigación Biomédica en Red de Enfermedades Raras (CIBERER), 08003 Barcelona, Spain
[3]Institució Catalana de Recerca i Estudis Avançats (ICREA), 08003 Barcelona, Spain
[4]These authors contributed equally to this work
[5]Present address: Department of Physiology, Development and Neuroscience, University of Cambridge, Cambridge CB2 3EG, United Kingdom
[6]Present address: Ludwig Institute for Cancer Research Stockholm Branch, Karolinska Institutet, SE-171 77 Stockholm, Sweden
[7]Present address: Division of Molecular Neurobiology, Department of Medical Biochemistry & Biophysics, Karolinska Institutet, SE-171 77 Stockholm, Sweden
[8]Present address: Instituto de Salud Carlos III, CNM, Área de Biología Celular y Desarrollo, Majadahonda 28220, Madrid, Spain
*Correspondence: mariona.arbones@crg.es (M.L.A.), isabel.farinas@uv.es (I.F.)
DOI 10.1016/j.stem.2010.06.021

SUMMARY

Stem cell division can result in two sibling cells exhibiting differential mitogenic and self-renewing potential. Here, we present evidence that the dual-specificity kinase Dyrk1A is part of a molecular pathway involved in the regulation of biased epidermal growth factor receptor (EGFR) signaling in the progeny of dividing neural stem cells (NSC) of the adult subependymal zone (SEZ). We show that EGFR asymmetry requires regulated sorting and that a normal *Dyrk1a* dosage is required to sustain EGFR in the two daughters of a symmetrically dividing progenitor. Dyrk1A is symmetrically or asymmetrically distributed during mitosis, and biochemical analyses indicate that it prevents endocytosis-mediated degradation of EGFR by a mechanism that requires phosphorylation of the EGFR signaling modulator Sprouty2. Finally, *Dyrk1a* heterozygous NSCs exhibit defects in self-renewal, EGF-dependent cell-fate decisions, and long-term persistence in vivo, suggesting that symmetrical divisions play a role in the maintenance of the SEZ reservoir.

INTRODUCTION

Asymmetric division allows stem cell pools to simultaneously self-renew and generate committed progeny, but it is becoming increasingly clear that stem cells modulate their numbers by switching between symmetrical and asymmetrical division modes (Morrison and Kimble, 2006). The subependymal zone (SEZ), adjacent to the lateral ventricles of the murine adult brain, is a very active germinal niche in which continual production of differentiated progeny is supported by a relatively quiescent population of astroglia/radial glia-like neural stem cells (NSC), named B cells. The progeny of glial fibrillary acidic protein (GFAP)-expressing B cells are transit-amplifying progenitor (TAP) cells, which rapidly divide and give rise to olfactory bulb (OB) local-circuitry neurons and to callosal oligodendrocytes (Zhao et al., 2008). In response to mitogenic stimuli, isolated SEZ cells produce clonal neurospheres, and long-term expansion of these cultures is considered an indication that symmetrical self-renewing divisions take place in vitro (Morshead and van der Kooy, 2004). Modes of division by adult NSCs in the SEZ, however, have not been extensively investigated. Horizontal and vertical cleavage planes with respect to the ventricle have been observed in dividing progenitors of the intact and ischemic SEZ, but whether symmetrical division modes occurred in B or TAP cells could not be determined (Zhang et al., 2004). Nevertheless, B cells exhibit properties of apicobasal polarity (Mirzadeh et al., 2008) and increase their numbers under certain conditions, suggesting that NSCs can divide symmetrically (Doetsch et al., 1999; Zhang et al., 2004).

Stem cell expansion in response to increased cellular demand suggests that niche signals modulate division mode, possibly acting on cell polarity factors and partitioning of fate determinants; in turn, differentially segregated molecules may function by altering gene expression and/or by modifying responsiveness to external cues in daughter cells. Molecules that regulate asymmetrical division in *Drosophila* neurogenesis are conserved in vertebrates; some of them exhibit polarized distribution in mammalian neural progenitor cells (NPC) and are involved in cell-fate decisions (Knoblich, 2008; Zhong and Chia, 2008). However, very little is known about the molecular players involved in determining biased signaling in adult mammalian stem cells. Recent studies have shown that epidermal growth factor receptor (EGFR) distribution varies between the siblings of fetal and adult NPCs and that inheritance of unequal receptor

amounts determines cell fate/potentiality (Sun et al., 2005; Andreu-Agulló et al., 2009). Unequal EGFR distribution is achieved by differential Notch-dependent transcription (Andreu-Agulló et al., 2009), but other possibilities, such as regulation of receptor trafficking, have not been evaluated.

Dyrk1A, a member of the dual-specificity tyrosine-phosphorylated and regulated kinase family, is expressed in developing and mature nervous systems (Martí et al., 2003; Hämmerle et al., 2008) and plays a role in brain growth. *DYRK1A* maps to the *Down syndrome critical region* of human chromosome 21, and its overexpression has been associated with some of the neurological defects observed in affected individuals (Park et al., 2009). *DYRK1A* dosage sensitivity is further highlighted by the fact that truncating mutations in hemizygosis result in microcephaly (Møller et al., 2008). Likewise, *Dyrk1a* loss-of-function mutations in *Drosophila* (*minibrain*) and mice result in defective neurogenesis (Tejedor et al., 1995; Fotaki et al., 2002). Dyrk1A phosphorylates substrates as diverse as microtubule-associated protein tau, caspase-9, Sprouty2 (Spry2), intracellular domain of Notch, or Shh effector Gli1, suggesting a possible role as signaling integrator (Galcerán et al., 2003; Aranda et al., 2008; Laguna et al., 2008; Fernandez-Martinez et al., 2009). Notably, *Dyrk1a* mRNA exhibits a polarized distribution in dividing neuroepithelial cells of the chick and mouse neural tubes (Hämmerle et al., 2002; 2008). Together, these data suggest a conserved essential role of Dyrk1A in neural development and, possibly, in asymmetric division.

We show here that Dyrk1A is expressed by B and TAP cells of the SEZ and that a reduction in Dyrk1A levels negatively impacts on the persistence of NSCs in this niche, a defect that correlates with impaired self-renewal of *Dyrk1a* heterozygous cells in vitro in response to EGF. Dyrk1A distributes both symmetrically and asymmetrically during mitosis of neurosphere-initiating cells, and EGFR levels and distribution in daughter cells depend on the amount of inherited Dyrk1A. Our data support a role for Dyrk1A as an inhibitor of EGFR degradation acting in the same pathway as the EGF-signaling regulator Spry2. Finally, we demonstrate that cell-fate decisions in response to EGF are altered in *Dyrk1a* heterozygous mice. Altogether, our data indicate that the regulation of EGF biased signaling by Dyrk1A controls NSC maintenance and mobilization in the mammalian SEZ.

RESULTS

Dyrk1A Is Expressed by NPCs of the Adult SEZ and Regulates NSC Longevity

Dyrk1A distribution in the murine adult brain had been previously analyzed (Martí et al., 2003), but expression in neurogenic regions was not reported. We detected Dyrk1A in SEZ and neurosphere homogenates by immunoblot and in all cells of the ependymal layer and in subependymal GFAP$^+$ cells and Mash1$^+$ TAP cells, but not in βIII-tubulin$^+$ neuroblasts, by immunohistochemistry (Figures 1A and 1B and Figures S1A–S1F). Dyrk1A was observed in GFAP$^+$ cells positive for the stem cell marker Sox2 and in cells that retained bromo-deoxyuridine for one month (BrdU label-retaining cells, BrdU-LRCs) (Figures 1C and 1D). "Activated" proliferative GFAP$^+$ B cells express EGFR (Doetsch et al., 2002; Pastrana et al., 2009), and virtually all GFAP$^+$/EGFR$^+$ cells (29 ± 2% of all GFAP$^+$ cells, n = 3) were positive for Dyrk1A (Figure 1E). We could also detect Dyrk1A in dividing GFAP$^+$ cells; notably, in some late mitoses, one daughter had detectable levels of Dyrk1A, whereas the other one hardly displayed any staining (Figures 1F and 1G and Movie S1), suggesting unequal Dyrk1A inheritance in NSC daughters (see also Figures S1G and S1H and Movie S2).

We next explored potential roles of Dyrk1A in the SEZ of 3-month-old (3-m) *Dyrk1a*$^{+/-}$ mice with reduced levels of the kinase (Figures 1A and 1B). These mice exhibit reduced brain size (Fotaki et al., 2002) and SEZ volumes (*Dyrk1a*$^{+/+}$: 0.037 ± 0.001 mm^3; *Dyrk1a*$^{+/-}$: 0.025 ± 0.002 mm^3; n = 5, $p < 0.05$; 32% reduction) and reduced densities of GFAP$^+$ and GFAP$^+$/Sox2$^+$ cells, but not of Mash1$^+$ TAP cells or βIII-tubulin$^+$ neuroblasts (Figures 2A and 2B). Likewise, the proliferative activity of GFAP$^+$ cells, but not of Mash1$^+$ cells or neuroblasts, was reduced in *Dyrk1a* mutants, suggesting specific effects of the mutation in B cells (Figures 2A and 2B). The lack of differences in BrdU/Ki67 ratio between genotypes (*Dyrk1a*$^{+/+}$: 76.7 ± 7.4%; *Dyrk1a*$^{+/-}$: 75.6 ± 1.5%; n = 3; Figure 2A) suggested that *Dyrk1a* heterozygosity does not result in an overall alteration of cell-cycle parameters in the SEZ but in fewer proliferating B cells.

Consistently, primary neurosphere yield was reduced in 3-m *Dyrk1a*$^{+/-}$ mice (Figures 2C and 2D; a small non-statistically significant reduction was observed at 2-m). Moreover, the difference in primary neurospheres between *Dyrk1a*$^{+/+}$ and *Dyrk1a*$^{+/-}$ mice steadily increased with age (Figure 2D) without further reductions in SEZ volume (*Dyrk1a*$^{+/+}$: 0.042 ± 0.008 mm^3; *Dyrk1a*$^{+/-}$: 0.027 ± 0.004 mm^3; n = 5 at 12-m, $p < 0.05$; 35% reduction). In contrast, no differences were detected in primary sphere yields from the SEZ of 4 day pups (*Dyrk1a*$^{+/+}$: 1280 ± 160; *Dyrk1a*$^{+/-}$: 1340 ± 105; n = 4), indicating that normal levels of Dyrk1A are not required for the generation of adult progenitors but for their life-long maintenance.

Reduced Expression of Dyrk1A Impairs EGF-Induced Self-Renewal In Vitro

The specific decrease in neurosphere recovery from *Dyrk1a*$^{+/-}$ SEZs suggested that normal levels of Dyrk1A are necessary for self-renewal. Accordingly, *Dyrk1a*$^{+/-}$ primary spheres grown in EGF + basic fibroblast growth factor (FGF) formed fewer secondary clones than wild-types (Figure 2E). Despite the difference in self-renewal, wild-type and *Dyrk1a*$^{+/-}$ cells did not differ in proliferation, cytokinesis, and apoptosis rates during the first passages, although defects in proliferation and progressive exhaustion were noticeable in *Dyrk1a*$^{+/-}$ cultures after passage 5 (Figures S2A–S2F). Therefore, a reduction in the frequency of symmetrical divisions in neurosphere-forming cells appears to be the primary phenotype of *Dyrk1a* haploinsufficiency.

Acute reduction of *Dyrk1a* expression in wild-type cells by siRNA also resulted in decreased neurosphere numbers, which could be partially reverted by retroviral delivery of a siRNA-resistant DYRK1A cDNA (Figure S2G). In contrast, overexpression of Dyrk1A did not affect neurosphere formation, as wild-type cells infected with a DYRK1A-containing retrovirus or cells from the SEZs of transgenic mice overexpressing *Dyrk1a* (Altafaj et al., 2001) formed the same number of neurospheres as their corresponding control cells (Figures S2G and S2H). Moreover, coculture experiments using transwell inserts with semipermeable

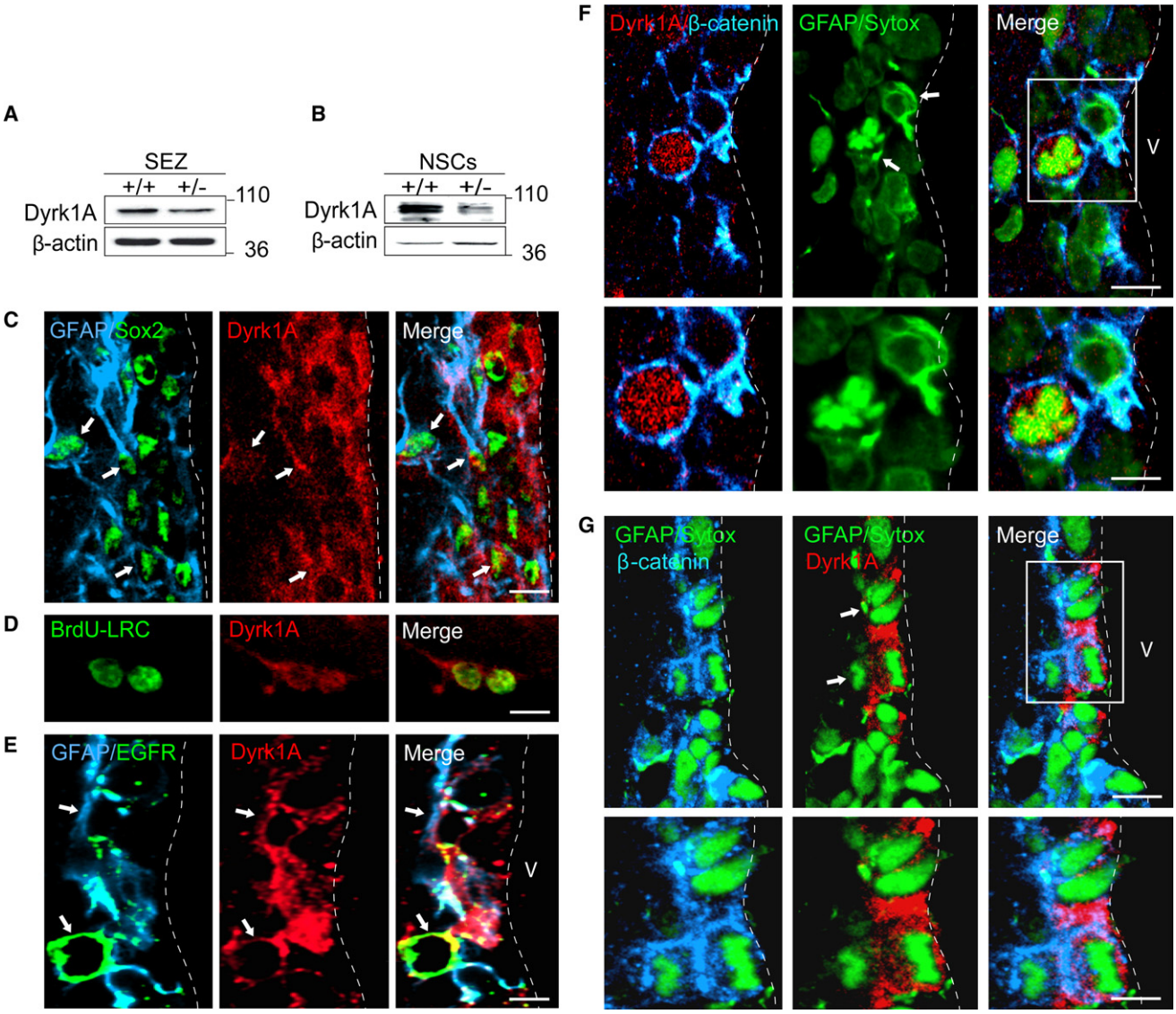

Figure 1. Expression of Dyrk1a in the Adult SEZ

Dyrk1A and β-actin in SEZ (A) and neurosphere (B) homogenates from wild-type (WT, +/+) and *Dyrk1a* heterozygous (+/−) mice by immunoblotting. (C) GFAP, Sox2, and Dyrk1A immunodetections. White arrows point at triple-positive cells. (D) Dyrk1A in BrdU-LRCs. (E) EGFR, GFAP, and Dyrk1A immunodetections. White arrows point at triple-positive cells. (F) Dividing GFAP$^+$ cell with membrane labeling for β-catenin and homogenous cytoplasmic staining for Dyrk1A. White arrows point at GFAP$^+$ processes. (G) Recently divided cells (white arrows) stained for GFAP, Dyrk1A, and β-catenin. Sytox Green labels nuclei. Bottom rows show higher magnification of cells in the white square. See rotations of the stacked confocal planes in Movie S1. Scale bars in (C) and (E), 20 μm; (D), 10 μm. (F) and (G): upper panels, 20 μm; lower panels, 10 μm.
See also Figure S1 and Movie S2.

membranes showed that *Dyrk1a*$^{+/-}$ cells did not modify the number of neurospheres formed by wild-type cells (Figure S2I), suggesting that Dyrk1A acts cell-autonomously to regulate self-renewal.

Next, *Dyrk1a*$^{+/-}$ and wild-type dissociated SEZs were cultured in medium with either EGF or FGF, and primary neurospheres formed under each condition were dissociated and plated separately in EGF or FGF. *Dyrk1a*$^{+/-}$ neurospheres grown in EGF yielded fewer secondary clones in either EGF or FGF than their wild-type counterparts. In contrast, secondary sphere formation did not differ between genotypes when cells had been grown in FGF (Figure 2F), indicating that normal Dyrk1A levels are specifically needed for EGF-induced symmetrical divisions.

Dyrk1A Protein Is Segregated during NSC Division and Regulates EGFR Distribution in Daughters

Dividing adult NSCs generate two daughters with asymmetric distribution of EGFR (EGFR^A; one cell with high and one cell with low EGFR levels) or two siblings with equal, symmetric, levels of EGFR (EGFR^S) (Andreu-Agulló et al., 2009). Immunocytochemistry in cell pairs showed that EGFR always colocalized

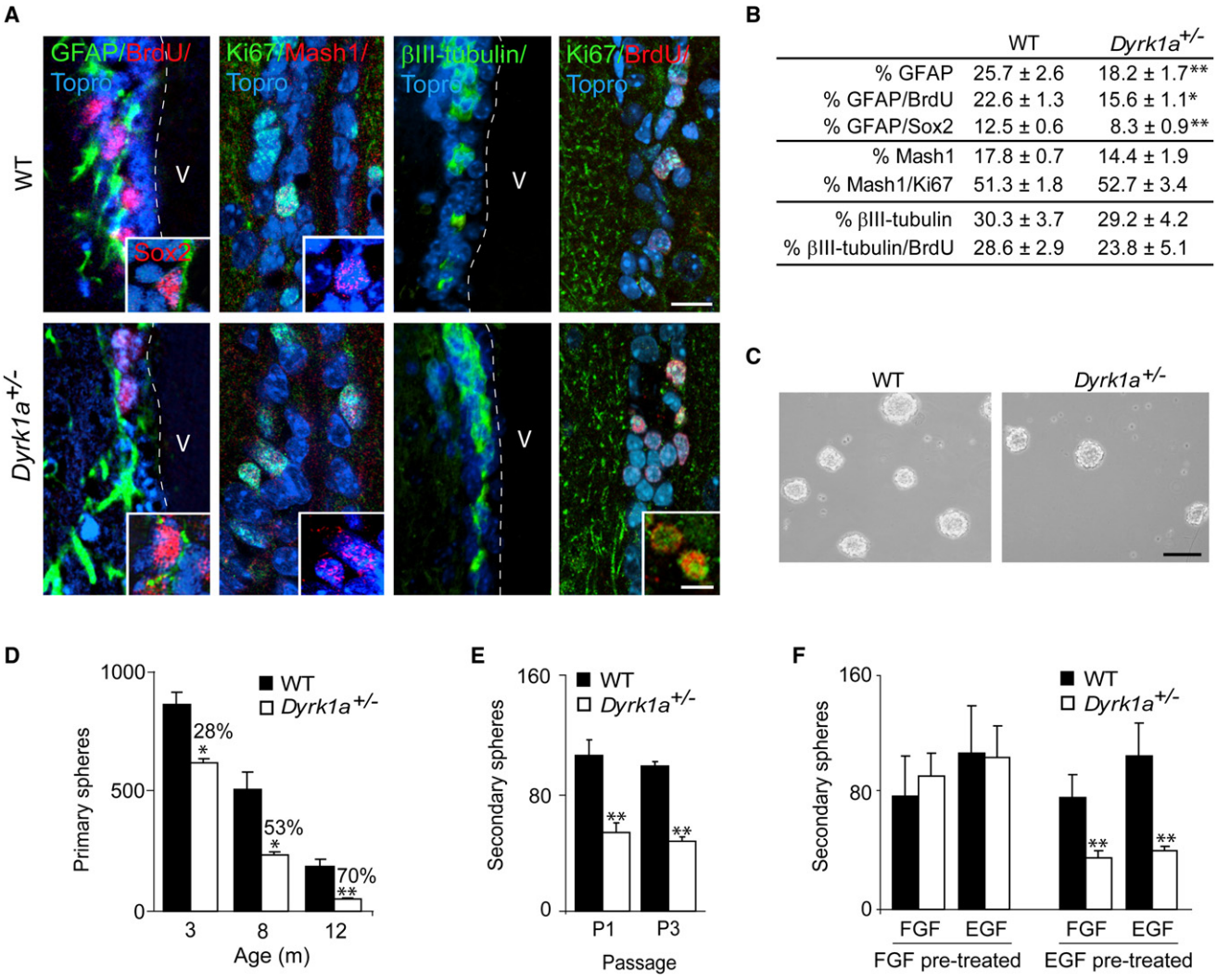

	WT	*Dyrk1a*$^{+/-}$
% GFAP	25.7 ± 2.6	18.2 ± 1.7**
% GFAP/BrdU	22.6 ± 1.3	15.6 ± 1.1*
% GFAP/Sox2	12.5 ± 0.6	8.3 ± 0.9**
% Mash1	17.8 ± 0.7	14.4 ± 1.9
% Mash1/Ki67	51.3 ± 1.8	52.7 ± 3.4
% βIII-tubulin	30.3 ± 3.7	29.2 ± 4.2
% βIII-tubulin/BrdU	28.6 ± 2.9	23.8 ± 5.1

Figure 2. Dyrk1A Regulates Self-Renewal

(A) Immunofluorescence for GFAP and BrdU (GFAP and Sox2 in the inset), Mash1 and Ki67, βIII-tubulin, and Ki67 and BrdU in BrdU-injected WT and *Dyrk1a*$^{+/-}$ mice. Topro-3 labels nuclei. Dashed white lines indicate the limits of the lateral ventricle (V).

(B) Density and proliferative activity of GFAP^{+} B cells, Mash1^{+} TAP cells, and βIII-tubulin neuroblasts.

(C) Passage (P) 1 secondary neurospheres.

(D) Primary sphere yields from 3-, 8-, and 12-m mice in EGF+FGF. Percent reductions in *Dyrk1a*$^{+/-}$ versus *Dyrk1a*$^{+/+}$ cultures are indicated.

(E) Secondary spheres formed in WT and *Dyrk1a*$^{+/-}$ cultures at P1 and P3.

(F) Secondary spheres formed in the presence of EGF or FGF by cells dissociated from primary neurospheres that had been previously grown in either EGF or FGF. Scale bars in (A), 20 μm; insets, 10 μm.

See also Figure S2.

with the marker of apical polarity atypical protein kinase C (aPKC) λ (Figure S3A). Moreover, unequal inheritance of EGFR led to a differential capacity for neurosphere formation, as cells with higher EGFR levels (sorted by FACS following incubation with Alexa 488-conjugated EGF) formed 2-fold more neurospheres than the population with low EGFR levels (Figure S3B).

Dyrk1A protein was also asymmetrically or symmetrically distributed in daughters of a dividing neurosphere-initiating cell and always detected in cells with high EGFR levels (Figure 3A). Asymmetric segregation of Dyrk1A could not be observed until telophase or cytokinesis, suggesting that Dyrk1A is unlikely to act as an early polarity determinant, but its asymmetric segregation appeared to precede that of EGFR (Figure 3B). To investigate whether asymmetrical distribution of Dyrk1A could be the result of an active partitioning of Dyrk1A in the dividing cell, we treated dissociated neurosphere cells with latrunculin A, a drug that disrupts the actin meshwork, preventing uneven distribution of asymmetric fate determinants (Sun et al., 2005). Treated cells exhibited a 60% reduction in Dyrk1A asymmetry (untreated, 32.2 ± 3.0%; treated, 11.7 ± 2.0%, n = 3, $p < 0.05$), an indication that Dyrk1A unequal distribution may depend on the actin cytoskeleton.

To analyze whether Dyrk1A haploinsufficiency affects EGFR distribution, we compared the frequency of EGFR^{A} and EGFR^{S}

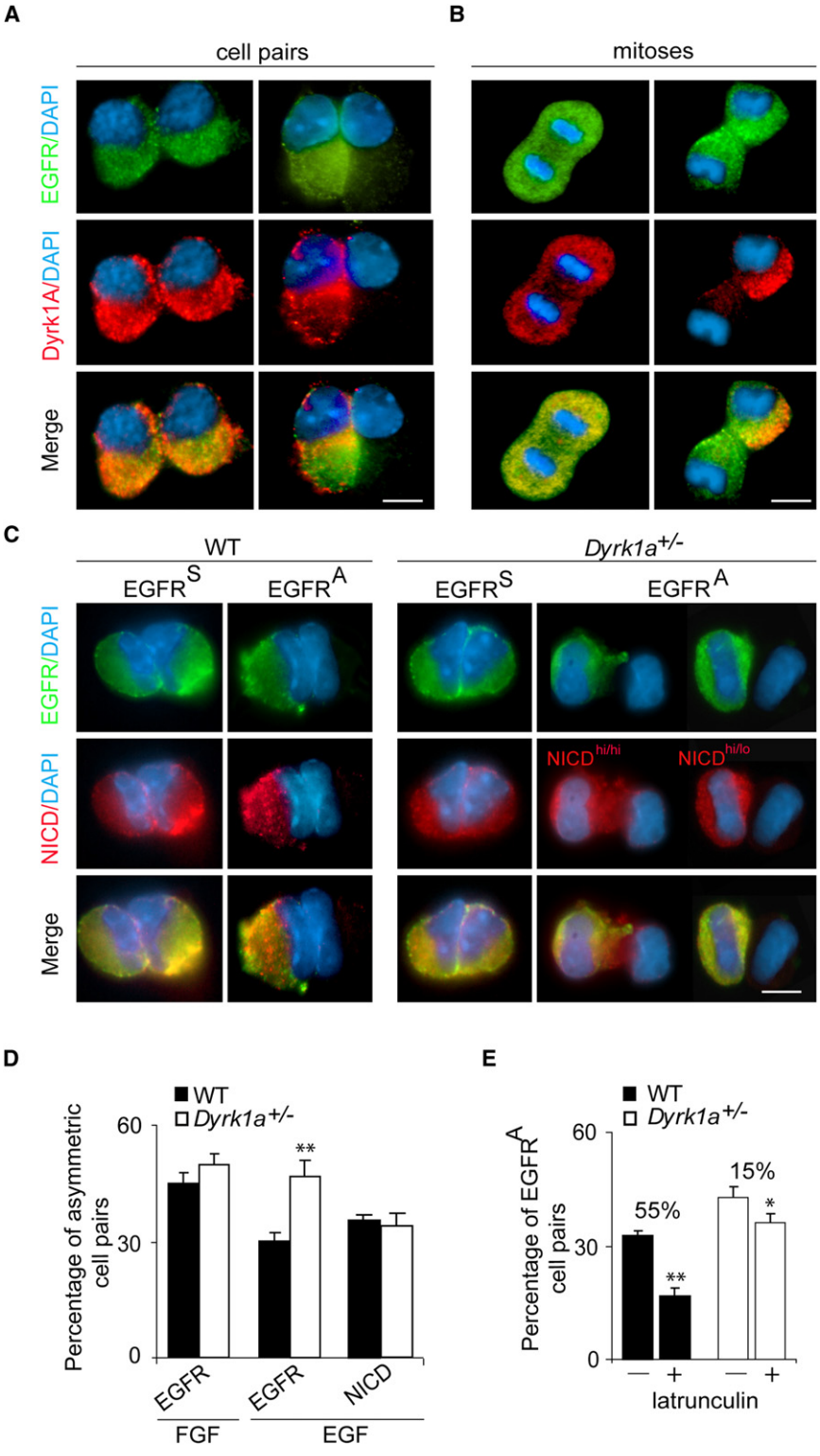

Figure 3. Mitotic EGFR and Dyrk1A Asymmetry

Dyrk1A and EGFR in cell pairs (A) and in late mitoses (B), showing symmetric and asymmetric codistribution. DAPI labels nuclei. (C) EGFR and NICD in WT and *Dyrk1a*$^{+/-}$ cell pairs. (D) Proportion of cell pairs with asymmetrical distribution of EGFR or NICD in WT and *Dyrk1a*$^{+/-}$ cells cultured in EGF or FGF. (E) Proportion of cell pairs with asymmetrical distribution of EGFR (EGFR^{A}) in WT and *Dyrk1a*$^{+/-}$ cells, either untreated (–) or treated (+) with latrunculin A. Scale bars in (A)–(C), 10 μm. See also Figure S3.

cell pairs in the two genotypes and found a significant increase in the relative proportion of EGFR^{A} cell pairs in *Dyrk1a*$^{+/-}$ cultures (Figures 3C and 3D). This increase occurred at the expense of EGFR^{S} doublets, since the proportion of cell pairs in which both cells were EGFR-low was not altered (*Dyrk1a*$^{+/+}$: 2.7 ± 0.5%; *Dyrk1a*$^{+/-}$: 3.1 ± 0.8%, n = 4). Notably, the increase in the EGFR^{A}/EGFR^{S} ratio was found in EGF, but not in FGF-treated cultures (Figure 3D), in agreement with the mitogen-dependent self-renewal defect. Noteworthy, overexpression of a GFP-Dyrk1A fusion protein in wild-type cells resulted in efficient asymmetrical segregation of both endogenous and ectopically expressed Dyrk1A and normal EGFR^{A}/EGFR^{S} ratio (Figures S3C and S3D), a result compatible with the observed unaltered self-renewal in Dyrk1A-overexpressing cultures.

Notch activity exhibits symmetric or asymmetric distribution in NSC daughters and positively correlates with EGFR expression and self-renewal potential (Andreu-Agulló et al., 2009), and immunostaining for the active Notch intracellular domain (NICD) showed a perfect match with EGFR and Dyrk1A distributions in *Dyrk1a*$^{+/+}$ cultures (Figure S3E). Since Dyrk1A heterozygous levels did not alter the proportion of NICD asymmetric cell pairs (Figure 3D), it appeared that normal Dyrk1A levels are required to sustain bilateral EGFR expression/maintenance in Notch-symmetric divisions. Therefore, we reasoned that any manipulation forcing a homogeneous distribution of Dyrk1A in dividing cells would produce an increase in EGFR symmetry that would be less apparent in heterozygous than in wild-type cultures. Treatment with latrunculin A indeed resulted in a reduction in the EGFR^{A}/EGFR^{S} ratio of around 50% in wild-type cultures and of only 15% in *Dyrk1a*$^{+/-}$ cultures (Figure 3E), in line with the basal phenotype of the heterozygous condition and suggesting that EGFR distribution depend on the mitotic partitioning of Dyrk1A in the dividing NSC. Our data are

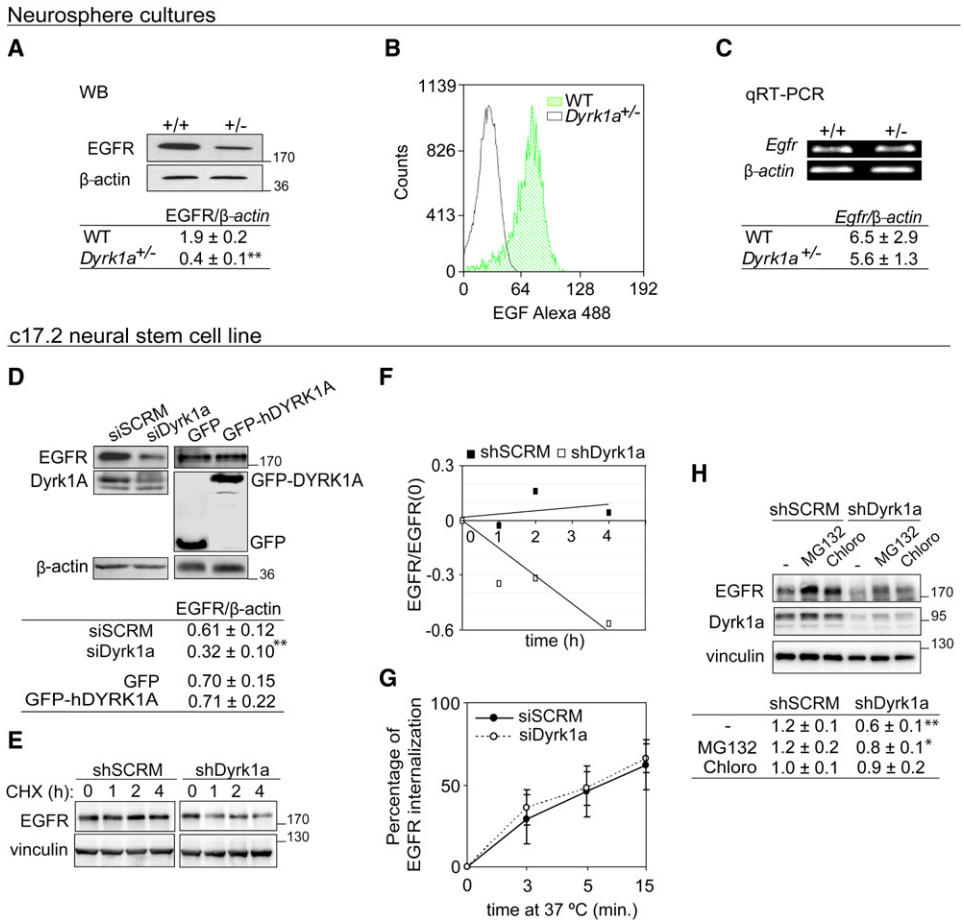

Figure 4. Dyrk1A Regulates EGFR Degradation in Neural Progenitors

(A) Relative EGFR/β-actin protein levels in WT (+/+) and *Dyrk1a*$^{+/-}$ (+/−) neurospheres.

(B) Representative flow cytometry scan showing cell distribution relative to Alexa 488-conjugated EGF fluorescence in WT and *Dyrk1a*$^{+/-}$ cells.

(C) *Egfr* mRNA in (+/+) and (+/−) cells and relative *Egfr*/*β-actin* levels assessed by qRT-PCR.

(D) Detection of EGFR, Dyrk1A, and GFP and EGFR/β-actin relative values in cells transduced with *Dyrk1a* (siDyrk1a) or scrambled (siSCRM) siRNA, or expressing unfused GFP or a GFP-DYRK1A fusion (GFP-hDYRK1A).

(E) EGFR stability time course in cells transduced with shDyrk1A or shSCRM and treated with cycloheximide (CHX) added 48 hr after transfection.

(F) Plot showing the natural log of normalized EGFR (EGFR/vinculin)/normalized EGFR at time zero.

(G) Internalization rate for the Alexa 488-EGF/EGFR complex in c17.2 cells nucleofected with *Dyrk1a* (siDyrk1a) or scrambled (siSCRM) siRNA.

(H) EGFR immunoblot and relative EGFR/vinculin levels in cells transfected with shDyrk1A or shSCRM and incubated with MG132 or chloroquine (Chloro) in the presence of CHX.

See also Figure S4.

compatible with a model in which 1/4 the normal (wild-type) dose is the minimum amount of Dyrk1A in a cell needed to support EGFR levels and, therefore, small stochastic variations in the homogeneous (symmetric) distribution of heterozygous levels between two daughters leads to maintenance of EGFR levels in only one of the cells (see proposed model in Figure S3F).

Dyrk1A Inhibits EGFR Degradation

Because our genetic data suggested that a minimum amount of Dyrk1A is needed to preserve EGFR levels, we next set out to get a mechanistic insight into the role of Dyrk1A. In heterozygous cultures, total and surface EGFR protein steady-state levels were reduced but *Egfr* mRNA levels were not affected (Figures 4A–4C), suggesting that Dyrk1A contributes to the maintenance of normal levels of membrane-bound EGFR by actions on EGFR posttranscriptional regulation.

As a first step toward the biochemical mechanism, we analyzed EGFR levels in cells of the c17.2 murine neural stem cell line (Snyder et al., 1992) with modified amounts of Dyrk1A. EGFR protein levels were not modified by Dyrk1A overexpression but became lower when Dyrk1A was reduced with a specific siRNA (Figure 4D). To determine whether the effects were due to enhanced degradation, the half-life of EGFR was estimated in cells treated with the protein synthesis inhibitor cycloheximide. EGFR levels were significantly decreased in Dyrk1A knocked-down cells during the cycloheximide chase (Figures 4E and 4F), suggesting that Dyrk1A antagonizes EGFR degradation.

EGFR endocytosis is a major mechanism to control EGF-dependent signaling and degradation/recycling (Sorkin and

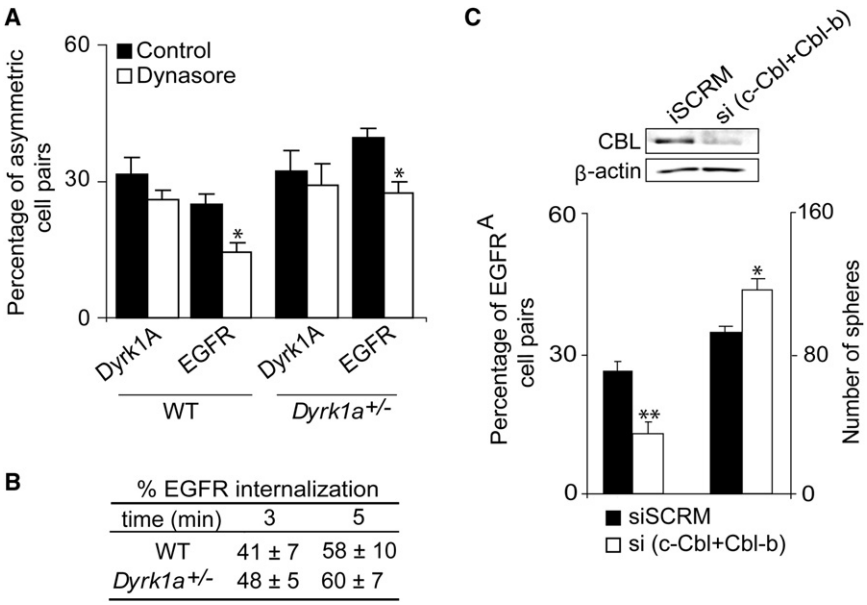

Figure 5. EGFR Asymmetric Distribution Requires Endocytosis-Mediated EGFR Degradation

(A) Percentage of EGFR and Dyrk1A asymmetric cell pairs in WT and *Dyrk1a*$^{+/-}$ cultures with and without (control) dynasore.

(B) Internalization rate for the Alexa 488-EGF/EGFR complex in WT and *Dyrk1a*$^{+/-}$ NSCs.

(C) Percentage of EGFR asymmetry in cell pairs and number of neurospheres formed by NSCs nucleofected with siSCRM and siRNAs to interfere Cbl-b and c-Cbl (the immunoblot illustrates the efficiency of the siRNA-knockdown).

von Zastrow, 2009). To investigate whether Dyrk1A maintained EGFR levels through actions on receptor internalization, we measured ligand/receptor internalization by flow cytometry. Quantification of the levels of internalized receptor, relative to initial surface levels, rendered no differences between c17.2 cells transfected with the Dyrk1A siRNA or with a scrambled siRNA (Figure 4G), an indication that Dyrk1A does not modulate EGFR internalization rates.

Once internalized, EGFR can either be recycled to the cell surface or targeted for degradation to late endosomes and lysosomes (Sorkin and von Zastrow, 2009). Addition of EGF to serum-starved c17.2 cells resulted in a time-dependent downregulation of EGFR protein levels, which was sensitive to lysosomal inhibitor chloroquine at early and late times post-stimulation and to proteasome inhibitor MG132 at early times (Figures S4A and S4B), indicating that both degradation pathways are active in these cells. The reduction in EGFR levels observed after EGF stimulation of Dyrk1A-interfered cells was rescued when the cultures were treated with chloroquine (Figure 4H), suggesting that normal levels of Dyrk1A antagonize lysosomal-mediated EGFR degradation. Altogether, our results indicated that Dyrk1A act as a brake for EGF-induced EGFR degradation in NPCs.

EGFR Asymmetry/Symmetry Is Dependent on EGFR Degradation following Internalization

To establish a link between EGFR stability and EGFR distribution in dividing cells, we focused on two processes associated with the regulation of EGFR half-life: endocytic internalization of ligand-receptor complexes and Cbl-dependent degradation. First, we treated singly dispersed NSCs with dynasore, a compound that hampers endocytosis by selectively inhibiting the GTPases dynamin 1 and 2 (Macia et al., 2006). Dynasore treatment did not modify the distribution of Dyrk1A but clearly inhibited the appearance of EGFR^{A} pairs in both wild-type and heterozygous cultures (Figure 5A), indicating that endocytosis plays a role in the unequal distribution of EGFR in NSC daughters. Similar to results in c17.2 cells, no differences were found between wild-type and *Dyrk1a*$^{+/-}$ cultures in EGFR internalization rate (Figure 5B). However, the dynasore treatment restored the proportion of EGFR^{A} in the heterozygous cultures to wild-type levels (Figure 5A), an effect compatible with Dyrk1A regulating EGFR levels and distribution at a step downstream of receptor internalization.

To provide evidence that asymmetric EGFR distribution in NSCs requires efficient degradation, we interfered the EGFR-specific E3 ligase Cbl (c-Cbl and Cbl-b isoforms), a key player in mediating EGFR downregulation (Levkowitz et al., 1998). Cbl knockdown decreased the EGFR^{A}/EGFR^{S} cell pair ratio and increased neurosphere formation when interfered cells were passaged (Figure 5C). This result is consistent with the proposal that asymmetric EGFR distribution in NSCs requires efficient degradation upon ligand-mediated receptor internalization.

EGFR Asymmetry/Symmetry Is Dependent on Dyrk1A-Dependent Phosphorylation of EGFR-Signaling Regulator Spry2

To achieve some molecular understanding on how the effects of Dyrk1A on the regulation of EGFR stability modulate EGFR distribution, we decided to focus on Dyrk1A substrates. The dynasore results excluded Dyrk1A substrates directly related with endocytosis, such as dynamin or amphiphiysin (Murakami et al., 2009). However, we have recently identified Spry2 as a Dyrk1A substrate (Aranda et al., 2008) and considered it a likely candidate to mediate Dyrk1A effects. Sprouty proteins (Spry1 to 4 in mammals) are modulators of receptor tyrosine kinases-dependent signaling in a cell-context-specific manner. In particular, Spry2 is able to enhance EGF-dependent signaling by reducing receptor ubiquitination and the trafficking of EGFR-containing vesicular bodies from early to late endosomes (Mason et al., 2006; Kim et al., 2007). Indeed, Spry2 interference in c17.2 cells led to a reduction in EGFR levels (Figure S5A), an indication that Spry2, like Dyrk1A, positively contributes to EGFR stabilization. Expression data were also compatible with a putative role of Spry2 in the SEZ; among all four Spry proteins, Spry2 was highly expressed in SEZ tissue and the only one detected in adult neurosphere cultures (Figure 6A). Moreover, GFAP^{+} cells of the SEZ

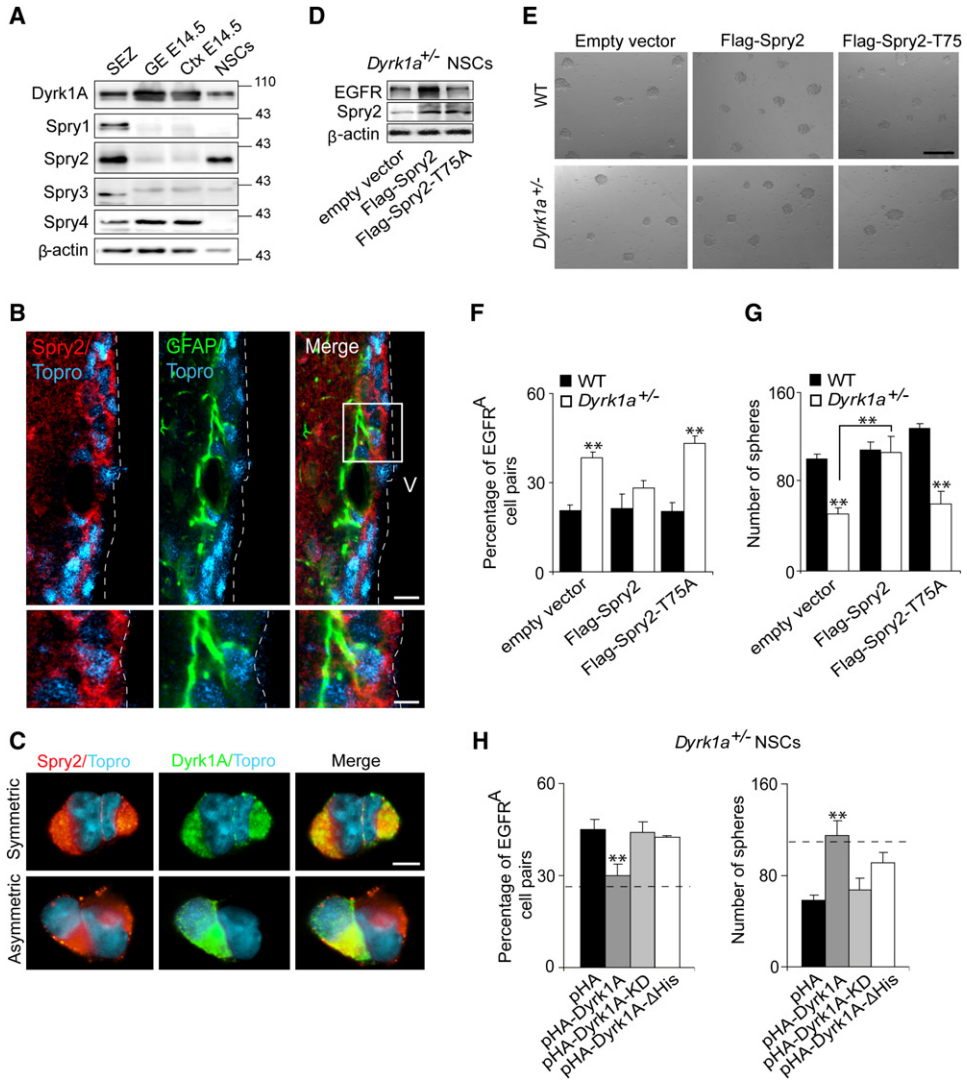

Figure 6. Dyrk1A Effects on EGFR Are Mediated by Phosphorylation of Spry2

(A) Detection of Spry proteins in adult SEZ, ganglionic eminences (GE), or cerebral cortex (Ctx) from E14.5 embryos, and adult neurosphere P4 cultures (NSCs) by immunoblot.

(B) GFAP and Spry2 in adult SEZ.

(C) Spry2 and Dyrk1A in cell pairs. Topro-3 (B) and DAPI (C) label nuclei.

(D) Spry2 and EGFR in lysates from *Dyrk1a*$^{+/-}$ cells expressing Flag-Spry2 or the T75A-mutated Spry2 version.

(E) Neurospheres growing from WT and *Dyrk1a*$^{+/-}$ cells nucleofected with the indicated constructs.

(F and G) Cell pairs with EGFR asymmetry (F) and number of neurospheres (G) in the same cultures as in (E).

(H) EGFR asymmetric cell pairs and sphere number in *Dyrk1a*$^{+/-}$ cultures expressing HA-DYRK1A, a kinase-deficient version (HA-DYRK1A-KD), or a version lacking the region that interacts with Spry2 (HA-DYRK1A-ΔHIS). The dashed line indicates the proportion of asymmetry and sphere numbers in WT cultures. Scale bars in (B): upper panels, 30 μm; lower panels, 10 μm; (C), 10 μm; (E), 100 μm.

See also Figure S5.

and cultured NSCs exhibited detectable levels of Spry2 although, unlike Dyrk1A or EGFR, Spry2 is not asymmetrically distributed in NSC daughters (Figures 6B and 6C).

We first interfered endogenous Spry2 in wild-type cells to explore whether Spry2 could regulate EGFR asymmetry and observed increased EGFR^{A}/EGFR^{S} cell pair ratios (Figure S5B), suggestive of a Spry2 involvement in the emergence of biased EGF signaling. We next tested whether Dyrk1A and Spry2 could be acting on the same pathway by overexpressing Spry2 in *Dyrk1a* heterozygous neurospheres. Exogenously expressed Spry2 significantly rescued the *Dyrk1a* heterozygous phenotype, as it resulted in increased EGFR protein levels, reduced EGFR^{A}/EGFR^{S} cell pair ratio, and higher neurosphere yield (Figures 6D–6G). In contrast, we were unable to restore wild-type proportions of EGFR^{A} cell pairs and neurosphere numbers in *Dyrk1a*$^{+/-}$ cultures by ectopic expression of a Spry2-mutated version in which the threonine residue that is phosphorylated by Dyrk1A was substituted by alanine (Spry2-T75A) (Aranda et al., 2008)

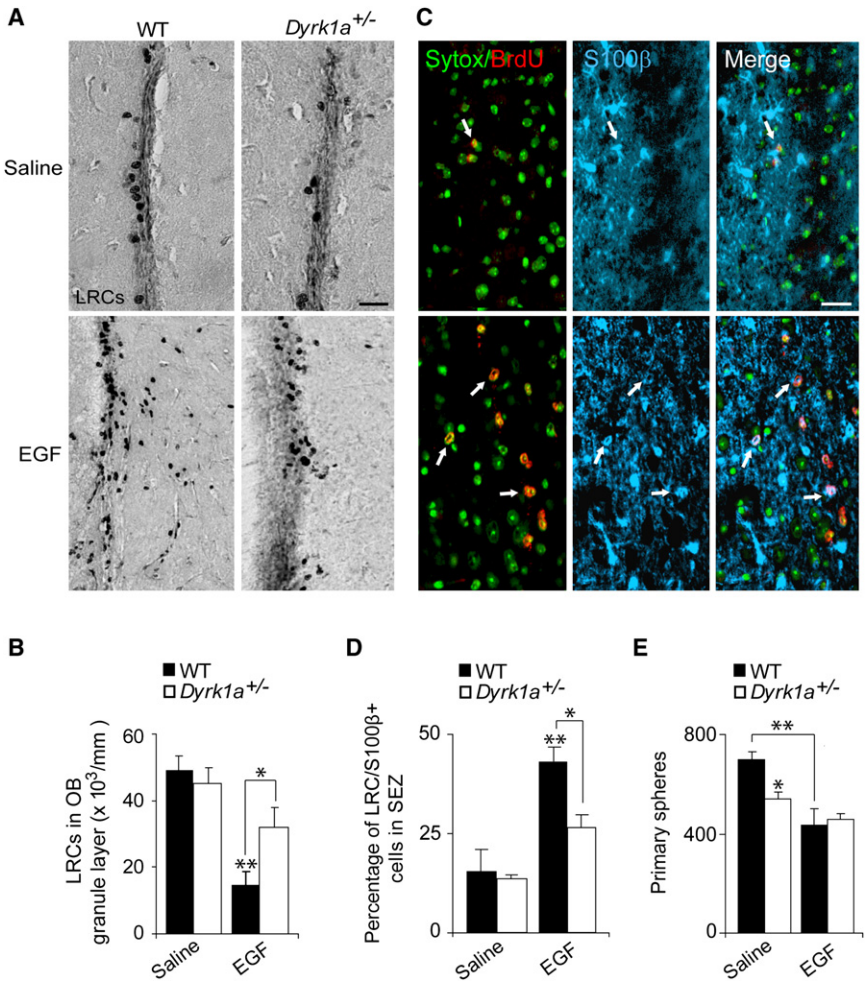

Figure 7. Dyrk1A Expression Levels Regulate EGF-Dependent NSC Fate Decisions In Vivo

(A) BrdU-LRCs in the SEZ of WT and *Dyrk1a*$^{+/-}$ saline- and EGF-infused mice.

(B) BrdU-LRC density in the OB granular layer of WT and *Dyrk1a*$^{+/-}$ mice 1 month after the infusion.

(C) Examples of S100β and BrdU detections in the striata of EGF- and saline-infused mice 1 month after EGF infusion. Nuclei are stained with Sytox.

(D) S100β^{+} BrdU-LRCs in the SEZ of WT and *Dyrk1a*$^{+/-}$ mice 1 month after the infusion.

(E) Neurosphere yield from WT and *Dyrk1a*$^{+/-}$ mice 1 month after the infusion. Scale bars in (A) and (C), 10 μm.

(Figures 6D–6G), suggesting that the rescuing effect of Spry2 overexpression on EGFR symmetry requires phosphorylation by Dyrk1A.

To test this proposal, wild-type neurosphere cultures were treated with the alkaloid harmine, a specific inhibitor of Dyrk1A kinase activity, and with norharmane, an analog alkaloid that does not inhibit Dyrk1A (Laguna et al., 2008). Only harmine treatment reproduced the heterozygous phenotype as it increased the proportion of EGFR^{A} cell pairs (norharmane, 30.6 ± 4.4; harmine, 55.4 ± 3.8; n = 3, $p < 0.05$). Furthermore, EGFR^{A}/EGFR^{S} ratio and sphere number were restored to normal values when *Dyrk1a*$^{+/-}$ cells were nucleofected with Dyrk1A, but not with a kinase-defective version (Dyrk1A-KD) or a mutated Dyrk1A that is catalytically active but cannot interact with Spry2 (Dyrk1A-ΔHis; Aranda et al., 2008) (Figure 6H). These results suggested that Dyrk1A phosphorylation of Spry2 is, at least, one mechanism by which Dyrk1A antagonizes EGFR degradation.

Dyrk1A Expression Level Regulates EGF-Dependent NSC-Fate Decisions In Vivo

We next decided to investigate whether NSC self-renewal and cell-fate decisions in response to EGF were also modified in *Dyrk1a* heterozygous tissue. It has reported that hyperproliferation of SEZ progenitors following infusion of EGF leads to reduced OB neurogenesis along with increased numbers of terminally differentiated astrocytes in the SEZ/striatum 1 month after the infusion (Craig et al., 1996; Kuhn et al., 1997; Doetsch et al., 2002). We therefore infused EGF for 7 days into the lateral ventricle of 2-m (before the heterozygous phenotype became evident) mice, injected them with BrdU on the last day of infusion, and one month later, analyzed BrdU labeling and neurosphere yield. The relative increase in the number of BrdU-LRCs cells in the brain of EGF versus saline-treated animals was similar between genotypes (around 10-fold) in wild-type (7014 ± 969 BrdU^{+} cells in EGF versus 785 ± 24 in saline, n = 4) and *Dyrk1a*$^{+/-}$ mice (5109 ± 431 in EGF versus 612 ± 17 in saline, n = 4), indicating that EGFR^{+} cells can be activated by acute EGF administration in both genotypes (Figure 7A). However, neurogenesis/astrogliogenesis and stem cell recovery 1 month after EGF infusion varied markedly between genotypes.

As reported, EGF infusion in wild-types resulted in reduced numbers of BrdU-LRCs in the OB granular layer and higher proportions of S100β^{+} BrdU-LRCs in the SEZ. Interestingly, both effects were less accentuated in *Dyrk1a*$^{+/-}$ mice (Figures 7B–7D). Given that S100β-labeling in the SEZ correlates with loss of neurosphere forming ability in vitro (Raponi et al., 2007), we next investigated whether the changes induced by EGF infusion correlated with a proliferation-driven exhaustion of stem cell potential by analyzing neurosphere recovery. EGF infusion indeed caused a reduction in the recovery of primary neurospheres in wild-type mice; in contrast, neurosphere recovery was the same from EGF- or saline-infused *Dyrk1a*$^{+/-}$ mice (Figure 7E). Together, these data suggested that Dyrk1A is an in vivo mediator of EGF-induced NSC decisions.

DISCUSSION

Endocytosis-mediated receptor degradation is emerging as a key regulator of polarized/asymmetric distribution of signaling

effectors within cells (i.e., for guided migration) or in sibling cells during cell division (i.e., for cell fate binary decisions) (Coumailleau and González-Gaitán, 2008). Our data identify Dyrk1A as a novel regulator of biased signaling in stem cells of the adult mammalian brain and suggest that intracellular trafficking and sorting of signaling receptors are also essential processes in the regulation of stem cell renewal. Dyrk1A protein is actively distributed during NSC division into its daughters and the inherited Dyrk1A acts as an inhibitor of EGFR degradation in a dosage-sensitive manner, determining the potential for neurosphere formation of each daughter cell. Biochemically, Dyrk1A antagonizes EGFR degradation after its internalization by, at least, phosphorylating the modulator of tyrosine kinase receptor signaling, Spry2.

The mechanism mediating Dyrk1A distribution remains unknown, although its sensitivity to latrunculin suggests that it may be cytoskeleton-dependent. Published work in embryonic NPCs indicates that *Dyrk1a* mRNA is asymmetrically localized during mitosis (Hämmerle et al., 2002; 2008), and it is thus possible that different amounts of protein are translated in daughter cells upon cell division, similarly to what occurs with some asymmetric determinants in *Drosophila* (Knoblich, 2008). The fact that a *Dyrk1a* cDNA without untranslated regions results in Dyrk1A asymmetric distribution points to the protein as the segregation target and suggests alternative possibilities, including the segregation of Dyrk1A associated to endosomal compartments, as it happens with the Notch-ligand Delta (Coumailleau and González-Gaitán, 2008). Other Dyrk family members control polarized growth and asymmetric cell division in yeast and nematodes, acting on the regulation of mitotic spindle positioning or on degradation-dependent asymmetric segregation of germ line determinants (Bähler and Nurse, 2001; Pang et al., 2004; Stitzel et al., 2006). Given that *minibrain* has been identified in a RNAi screen for cytokinesis defects and as a regulator of actin organization (Bettencourt-Dias et al., 2004; Liu et al., 2009), it remains to be determined whether Dyrk1A can directly regulate mammalian NSC division mode through additional actions on the cytoskeleton.

EGF-dependent biased signaling for self-renewal can be regulated at different levels. For instance, Notch activity is segregated during NSC division and directly regulates expression of the *Egfr* gene (Andreu-Agulló et al., 2009). Because Dyrk1A can antagonize EGFR degradation in cells with high Notch activity, both mechanisms likely contribute to increase EGF response. In contrast, increased probability of EGFR degradation versus recycling in the cell with low Notch/low Dyrk1A could enhance signaling differences between sibling cells. Although an inhibitory role for Dyrk1A on Notch transcriptional activity has been reported (Fernandez-Martinez et al., 2009), we have not observed changes in *Egfr* mRNA levels in *Dyrk1a* heterozygous cells and therefore Dyrk1A activity might not act through Notch in this cell context. Regulation of Notch activity by Numb in embryonic progenitors is a classic example of how the asymmetric partitioning of an intracellular trafficking modulator results in differential fate in sibling cells and it has been suggested that Numb terminates Notch-dependent signals by promoting Notch internalization and degradation through a yet-unknown mechanism (Knoblich, 2008; Zhong and Chia, 2008). Numb can also inhibit Shh signaling through Gli1 ubiquitination and subsequent degradation and is involved in EGFR internalization (Santolini et al., 2000; Di Marcotullio et al., 2006). Given that Shh, Notch and EGFR positively regulate stem cell self-renewal (Molofsky et al., 2004; Andreu-Agulló et al., 2009), Numb inheritance could be associated with loss of stem potential. *In Drosophila*, Numb localizes basally in dividing neuroepithelial cells, opposite to the localization of the PAR complex (Knoblich, 2008). In neurosphere cultures, NICD, Dyrk1A and EGFR always segregate with the apical marker aPKCλ, suggesting that they could all be components of a self-renewal promoting machinery.

Our biochemical results indicate that Dyrk1A acts, at least in part, through binding to and phosphorylation of Spry2. Potentially, this phosphorylation could regulate Spry2 binding to trafficking regulatory proteins similarly to what has been described for Spry2 serine residues 112 and 121 (Kim et al., 2007). We have shown that phosphorylation of Spry2 on Thr75 by Dyrk1A impairs its inhibitory action on FGF-induced mitogen-activated protein kinase activation (Aranda et al., 2008) and our present data indicate that the same phosphorylation event contributes to EGFR accumulation in neurosphere cells. Although neurosphere cells are responsive to other mitogens, such as FGF or PDGF (Molofsky et al., 2004), FGFR or PDGFR asymmetries are not modified by Dyrk1A genetic reduction and/or Spry2 overexpression in NSCs (Figure 5SC). Thus the impact of Spry2 phosphorylation on the responsiveness to specific mitogens may not equally result in changes in self-renewal capabilities, in line with the idea that Spry actions are growth factor- and tissue-specific (Kim and Bar-Sagi, 2004).

Given that a fraction of B astrocytes express high levels of EGFR and respond to infused EGF and that this mitogen is essential for the derivation and propagation of adult neurosphere cultures, it is likely that EGF-dependent signaling contributes to SEZ homeostasis. In this line, aged mice exhibit reductions in EGFR and TGFα levels and stem cell potential is reduced in TGFα hypomorphic mice (Enwere et al., 2004). Higher EGFR levels correlate with a higher efficacy in neurosphere formation and NPCs derived from the postnatal and adult SEZ are enriched in neurosphere forming cells when sorted for high EGFR (Ciccolini et al., 2005; Pastrana et al., 2009). Moreover, Notch transcriptional activity correlates with self-renewal and promotes EGFR expression (Andreu-Agulló et al., 2009). Therefore, physical EGFR asymmetry could result in functional asymmetry and underlie the reduced longevity of the stem cell pool in *Dyrk1a* heterozygous mice. Finally, our observation that EGF-induced hyperproliferation results in a loss of stem cell potential and of neurogenesis in wild-type animals, but not in *Dyrk1a* heterozygous mutants, suggests that a fine balance between symmetrical and asymmetrical divisions is important to avoid depletion of the SEZ stem cell reservoir.

The human *DYRK1A* gene has been associated with DS neurological defects (Park et al., 2009). Although transient ectopic expression of Dyrk1A in NPCs of the developing fetal cortex results in premature differentiation (Yabut et al., 2010), we have observed that a moderate increase in Dyrk1A levels has no apparent effects on adult NSC behavior. Dose-dependent effects of Dyrk1A both in human pathology and rodent NPCs support that maintenance of a correct Dyrk1A dose is extremely important to preserve normal neurogenesis, both during development and in the adult.

EXPERIMENTAL PROCEDURES

Animal Use

Dyrk1a mutant mice (Altafaj et al., 2001; Fotaki et al., 2002) were used in accordance with institutional guidelines. BrdU (Sigma) was injected intraperitoneally (50 mg/g body weight) every 2 hr for a 12 hr period, and mice were either sacrificed immediately or 4 weeks later (to label LRCs). Infusion (7 days at a flow rate of 0.5 μl/h; 400 ng EGF/day) and fixation methods with 4% paraformaldehyde have been described (Ferrón et al., 2007).

Neurosphere Cultures, Treatments, and Cell-Pair Analysis

Methods for NSC culture, self-renewal assessment, and cell-pair analysis have been described (Ferrón et al., 2007; Andreu-Agulló et al., 2009). Isolated cells were incubated with latrunculin A (50 nM, Sigma), harmine (20 nM, TCI Europe), or norharmane (20 nM, Sigma) for 90 min, washed, seeded in growth medium, and fixed 12 hr later. Cells were treated with dynasore (40 nM, Sigma) for 4 hr at 16 hr after dissociation.

Immunostaining

Vibratome sections (30 μm) or cells/neurospheres were immunostained as described (Ferrón et al., 2007; see Table S1 for antibody details). Biotinylated *Griffonia simplicifolia* IB4 lectin (Sigma) was used at 1:20 and detected with Cy2-conjugated streptavidin (Jackson Immunochemicals, 1:1000). DAPI (1 mg/ml), Sytox Green, or Topro-3 (1:1000; Molecular Probes) were used (5 min) for nuclei counterstaining. Sections were incubated in 2 N HCl for 30 min at 37°C and neutralized in 0.1 M sodium borate (pH 8.5) before addition of BrdU antibodies. In some sections, a biotinylated anti-mouse antibody (1:200; Vector Labs) was used followed by the ABC complex (Vector Labs) reacted with 0.03% diaminobenzidine (Sigma) and 0.003% hydrogen peroxide. Immunoperoxidase-reacted sections were used for unbiased stereological counts of $BrdU^+$ LRCs with the optical dissector method (see Supplemental Information for details), using a CAST-GRID software package (Olympus, Denmark) adapted to an Olympus BX51 microscope.

Protein and RNA Isolation and Detection

Preparation of cell and tissue extracts, immunoblotting, and RT-PCR conditions have been previously described (Andreu-Agulló et al., 2009; see antibodies in Table S1). Real-time qPCR was performed in a DNA Engine 2 Opticon detection system (Bio-Rad) using SYBR Green I (see primer sequences in Table S2).

Cell Transduction

Neurospheres grown for 2 days were electroporated with DNAs or siRNAs (see Table S2 for sequences) using a Mouse NSC Nucleofector Kit (Amaxa Biosystems, Germany) or retrovirally infected, dissociated 2 days after transduction, and seeded at low-density. The retroviral vector pMSCV-puro (Clontech) was used to generate DYRK1A constructs (wild-type and the kinase inactive mutant DYRK1A/K179R, DYRK1A-KD); viral stocks were prepared by calcium phosphate transfection into the Phoenix helper-free cell line (ATCC). c17.2 cells (generously provided by E. Snyder) were cultured in Dulbecco's Modified Eagle's Medium (DMEM) plus 10% fetal bovine serum, 5% horse serum, 1% L-glutamine, and 1% sodium pyruvate. Cells were transfected with siRNAs (100 nM/35 mm plates) or DNAs (2 μg/35 mm plates) using Lipofectamine 2000 or Lipofectamine/plusReagent in Opti-MEM (Invitrogen), respectively, and processed after 24 hr (siRNA) or 48 hr (DNA). For the knockdown experiments, cells were cotransfected with pBABEpuro and selected with puromycin (1.2 μg/ml, Sigma). For EGFR degradation assays, c17.2 cells were serum starved for at least 2 hr, and 50 ng/ml EGF was added for the indicated periods of time. When required, cycloheximide (10 μg/ml), MG132 (10 μM), or chloroquine (200 μM) were added. Plasmids pBSU6-shDYRK1A and pBSU6-shSCRAMBLE and plasmids to express GFP-tagged DYRK1A, HA-tagged DYRK1A wild-type, a kinase inactive version and a mutant without the histidine repeat, and Flag-tagged Spry2 wild-type and T75A mutant versions have been described (Alvarez et al., 2003; Aranda et al., 2008; Ortiz-Abalia et al., 2008). A plasmid expressing a shRNA for Spry2 was kindly provided by D. Bar-Sagi (Kim et al., 2007).

EGFR Internalization

Cells were EGF-starved for 12 hr and incubated with 25 ng/ml Alexa Fluor 488-conjugated EGF at 4°C during 30 min. Low and high EGF populations were gated on the basis of a 30-fold increase in fluorescence levels with respect to control cells. Sorting was performed on a MoFlo sorter (Dako), and at least 200 cells from each population were plated at clonal density (1 cell/well) in neurosphere medium. For EGFR internalization analysis and after the incubation with Alexa Fluor 488-conjugated EGF, cells were rinsed three times with cold PBS, subjected to a cold acid-wash (DMEM, pH 2.2) for 5 min to remove noninternalized EGF, incubated at 37°C for the indicated times to allow internalization, and fixed. Fluorescence emission was detected by flow cytometry (MoFlo, Dako) and quantitated using the Sumit 4.0 software package (Dako).

Statistical Analysis

Analyses of significant differences were performed using the Student's t test. When comparisons were performed with relative values (normalized values and percentages), data were first normalized by using an arcsen transformation. Each experiment was performed in at least three independent cultures/animals per genotype and condition, and data are presented as mean ± SEM. A probability value of less than 5% was considered significant: $^{***}p < 0.001$; $^{**}p < 0.01$; $^{*}p < 0.05$.

SUPPLEMENTAL INFORMATION

Supplemental Information includes five figures, two tables, Supplemental Experimental Procedures, and two movies and can be found with this article online at doi:10.1016/j.stem.2010.06.021.

ACKNOWLEDGMENTS

We thank M.P. Rubio, U. Brandt-Bohne, and S. Turró for help with constructs, viral production, and immunoblotting; M.J. Palop and E. Ramírez for help with the mouse colonies; and S. Bartlett for English editorial work. This work was supported by grants from Ministerio de Ciencia e Innovación to I.F., M.L.A., P.S., and S.L.; from Ministerio de Sanidad y Consumo (CIBERNED and Red Tercel to I.F. and CIBERER and FIS04/1559 to C.F.); Generalitat Valenciana (Programa Prometeo) and Fundación "la Caixa" to I.F.; and the Jerôme Lejeune Foundation and the EU grant AnEUploidy to M.L.A. A.L. and S.A. were FI predoctoral fellows (DURSI, Generalitat de Catalunya).

Received: July 3, 2009
Revised: March 30, 2010
Accepted: June 4, 2010
Published: September 2, 2010

REFERENCES

Altafaj, X., Dierssen, M., Baamonde, C., Martí, E., Visa, J., Guimerà, J., Oset, M., González, J.R., Flórez, J., Fillat, C., and Estivill, X. (2001). Neurodevelopmental delay, motor abnormalities and cognitive deficits in transgenic mice overexpressing Dyrk1A (minibrain), a murine model of Down's syndrome. Hum. Mol. Genet. *10*, 1915–1923.

Alvarez, M., Estivill, X., and de la Luna, S. (2003). DYRK1A accumulates in splicing speckles through a novel targeting signal and induces speckle disassembly. J. Cell Sci. *116*, 3099–3107.

Andreu-Agulló, C., Morante-Redolat, J.M., Delgado, A.C., and Fariñas, I. (2009). Vascular niche factor PEDF modulates Notch-dependent stemness in the adult subependymal zone. Nat. Neurosci. *12*, 1514–1523.

Aranda, S., Alvarez, M., Turró, S., Laguna, A., and de la Luna, S. (2008). Sprouty2-mediated inhibition of fibroblast growth factor signaling is modulated by the protein kinase DYRK1A. Mol. Cell. Biol. *28*, 5899–5911.

Bähler, J., and Nurse, P. (2001). Fission yeast Pom1p kinase activity is cell cycle regulated and essential for cellular symmetry during growth and division. EMBO J. *20*, 1064–1073.

Bettencourt-Dias, M., Giet, R., Sinka, R., Mazumdar, A., Lock, W.G., Balloux, F., Zafiropoulos, P.J., Yamaguchi, S., Winter, S., Carthew, R.W., et al. (2004).

Genome-wide survey of protein kinases required for cell cycle progression. Nature *432*, 980–987.

Ciccolini, F., Mandl, C., Hölzl-Wenig, G., Kehlenbach, A., and Hellwig, A. (2005). Prospective isolation of late development multipotent precursors whose migration is promoted by EGFR. Dev. Biol. *284*, 112–125.

Coumailleau, F., and González-Gaitán, M. (2008). From endocytosis to tumors through asymmetric cell division of stem cells. Curr. Opin. Cell Biol. *20*, 462–469.

Craig, C.G., Tropepe, V., Morshead, C.M., Reynolds, B.A., Weiss, S., and van der Kooy, D. (1996). In vivo growth factor expansion of endogenous subependymal neural precursor cell populations in the adult mouse brain. J. Neurosci. *16*, 2649–2658.

Di Marcotullio, L., Ferretti, E., Greco, A., De Smaele, E., Po, A., Sico, M.A., Alimandi, M., Giannini, G., Maroder, M., Screpanti, I., and Gulino, A. (2006). Numb is a suppressor of Hedgehog signalling and targets Gli1 for Itch-dependent ubiquitination. Nat. Cell Biol. *8*, 1415–1423.

Doetsch, F., García-Verdugo, J.M., and Alvarez-Buylla, A. (1999). Regeneration of a germinal layer in the adult mammalian brain. Proc. Natl. Acad. Sci. USA *96*, 11619–11624.

Doetsch, F., Petreanu, L., Caille, I., García-Verdugo, J.M., and Álvarez-Buylla, A. (2002). EGF converts transit-amplifying neurogenic precursors in the adult brain into multipotent stem cells. Neuron *36*, 1021–1034.

Enwere, E., Shingo, T., Gregg, C., Fujikawa, H., Ohta, S., and Weiss, S. (2004). Aging results in reduced epidermal growth factor receptor signaling, diminished olfactory neurogenesis, and deficits in fine olfactory discrimination. J. Neurosci. *24*, 8354–8365.

Fernandez-Martinez, J., Vela, E.M., Tora-Ponsioen, M., Ocaña, O.H., Nieto, M.A., and Galcerán, J. (2009). Attenuation of Notch signalling by the Down-syndrome-associated kinase DYRK1A. J. Cell Sci. *122*, 1574–1583.

Ferrón, S.R., Andreu-Agullo, C., Mira, H., Sánchez, P., Marqués-Torrejon, M.A., and Fariñas, I. (2007). A combined ex/in vivo assay to detect effects of exogenously added factors in neural stem cells. Nat. Protoc. *2*, 849–859.

Fotaki, V., Dierssen, M., Alcántara, S., Martínez, S., Martí, E., Casas, C., Visa, J., Soriano, E., Estivill, X., and Arbonés, M.L. (2002). Dyrk1A haploinsufficiency affects viability and causes developmental delay and abnormal brain morphology in mice. Mol. Cell. Biol. *22*, 6636–6647.

Galcerán, J., de Graaf, K., Tejedor, F.J., and Becker, W. (2003). The MNB/DYRK1A protein kinase: genetic and biochemical properties. J. Neural Transm. Suppl. *67*, 139–148.

Hämmerle, B., Vera-Samper, E., Speicher, S., Arencibia, R., Martínez, S., and Tejedor, F.J. (2002). Mnb/Dyrk1A is transiently expressed and asymmetrically segregated in neural progenitor cells at the transition to neurogenic divisions. Dev. Biol. *246*, 259–273.

Hämmerle, B., Elizalde, C., and Tejedor, F.J. (2008). The spatio-temporal and subcellular expression of the candidate Down syndrome gene Mnb/Dyrk1A in the developing mouse brain suggests distinct sequential roles in neuronal development. Eur. J. Neurosci. *27*, 1061–1074.

Kim, H.J., and Bar-Sagi, D. (2004). Modulation of signalling by Sprouty: a developing story. Nat. Rev. Mol. Cell Biol. *5*, 441–450.

Kim, H.J., Taylor, L.J., and Bar-Sagi, D. (2007). Spatial regulation of EGFR signaling by Sprouty2. Curr. Biol. *17*, 455–461.

Knoblich, J.A. (2008). Mechanisms of asymmetric stem cell division. Cell *132*, 583–597.

Kuhn, H.G., Winkler, J., Kempermann, G., Thal, L.J., and Gage, F.H. (1997). Epidermal growth factor and fibroblast growth factor-2 have different effects on neural progenitors in the adult rat brain. J. Neurosci. *17*, 5820–5829.

Laguna, A., Aranda, S., Barallobre, M.J., Barhoum, R., Fernández, E., Fotaki, V., Delabar, J.M., de la Luna, S., de la Villa, P., and Arbonés, M.L. (2008). The protein kinase DYRK1A regulates caspase-9-mediated apoptosis during retina development. Dev. Cell *15*, 841–853.

Levkowitz, G., Waterman, H., Zamir, E., Kam, Z., Oved, S., Langdon, W.Y., Beguinot, L., Geiger, B., and Yarden, Y. (1998). c-Cbl/Sli-1 regulates endocytic sorting and ubiquitination of the epidermal growth factor receptor. Genes Dev. *12*, 3663–3674.

Liu, T., Sims, D., and Baum, B. (2009). Parallel RNAi screens across different cell lines identify generic and cell type-specific regulators of actin organization and cell morphology. Genome Biol. *10*, R26.

Macia, E., Ehrlich, M., Massol, R., Boucrot, E., Brunner, C., and Kirchhausen, T. (2006). Dynasore, a cell-permeable inhibitor of dynamin. Dev. Cell *10*, 839–850.

Martí, E., Altafaj, X., Dierssen, M., de la Luna, S., Fotaki, V., Alvarez, M., Pérez-Riba, M., Ferrer, I., and Estivill, X. (2003). Dyrk1A expression pattern supports specific roles of this kinase in the adult central nervous system. Brain Res. *964*, 250–263.

Mason, J.M., Morrison, D.J., Basson, M.A., and Licht, J.D. (2006). Sprouty proteins: multifaceted negative-feedback regulators of receptor tyrosine kinase signaling. Trends Cell Biol. *16*, 45–54.

Mirzadeh, Z., Merkle, F.T., Soriano-Navarro, M., Garcia-Verdugo, J.M., and Alvarez-Buylla, A. (2008). Neural stem cells confer unique pinwheel architecture to the ventricular surface in neurogenic regions of the adult brain. Cell Stem Cell *3*, 265–278.

Møller, R.S., Kübart, S., Hoeltzenbein, M., Heye, B., Vogel, I., Hansen, C.P., Menzel, C., Ullmann, R., Tommerup, N., Ropers, H.H., et al. (2008). Truncation of the Down syndrome candidate gene DYRK1A in two unrelated patients with microcephaly. Am. J. Hum. Genet. *82*, 1165–1170.

Molofsky, A.V., Pardal, R., and Morrison, S.J. (2004). Diverse mechanisms regulate stem cell self-renewal. Curr. Opin. Cell Biol. *16*, 700–707.

Morrison, S.J., and Kimble, J. (2006). Asymmetric and symmetric stem-cell divisions in development and cancer. Nature *441*, 1068–1074.

Morshead, C.M., and van der Kooy, D. (2004). Disguising adult neural stem cells. Curr. Opin. Neurobiol. *14*, 125–131.

Murakami, N., Bolton, D., and Hwang, Y.W. (2009). Dyrk1A binds to multiple endocytic proteins required for formation of clathrin-coated vesicles. Biochemistry *48*, 9297–9305.

Ortiz-Abalia, J., Sahún, I., Altafaj, X., Andreu, N., Estivill, X., Dierssen, M., and Fillat, C. (2008). Targeting Dyrk1A with AAVshRNA attenuates motor alterations in TgDyrk1A, a mouse model of Down syndrome. Am. J. Hum. Genet. *83*, 479–488.

Pang, K.M., Ishidate, T., Nakamura, K., Shirayama, M., Trzepacz, C., Schubert, C.M., Priess, J.R., and Mello, C.C. (2004). The minibrain kinase homolog, mbk-2, is required for spindle positioning and asymmetric cell division in early C. elegans embryos. Dev. Biol. *265*, 127–139.

Park, J., Song, W.J., and Chung, K.C. (2009). Function and regulation of Dyrk1A: towards understanding Down syndrome. Cell. Mol. Life Sci. *66*, 3235–3240.

Pastrana, E., Cheng, L.C., and Doetsch, F. (2009). Simultaneous prospective purification of adult subventricular zone neural stem cells and their progeny. Proc. Natl. Acad. Sci. USA *106*, 6387–6392.

Raponi, E., Agenes, F., Delphin, C., Assard, N., Baudier, J., Legraverend, C., and Deloulme, J.C. (2007). S100B expression defines a state in which GFAP-expressing cells lose their neural stem cell potential and acquire a more mature developmental stage. Glia *55*, 165–177.

Santolini, E., Puri, C., Salcini, A.E., Gagliani, M.C., Pelicci, P.G., Tacchetti, C., and Di Fiore, P.P. (2000). Numb is an endocytic protein. J. Cell Biol. *151*, 1345–1352.

Snyder, E.Y., Deitcher, D.L., Walsh, C., Arnold-Aldea, S., Hartwieg, E.A., and Cepko, C.L. (1992). Multipotent neural cell lines can engraft and participate in development of mouse cerebellum. Cell *68*, 33–51.

Sorkin, A., and von Zastrow, M. (2009). Endocytosis and signalling: intertwining molecular networks. Nat. Rev. Mol. Cell Biol. *10*, 609–622.

Stitzel, M.L., Pellettieri, J., and Seydoux, G. (2006). The C. elegans DYRK Kinase MBK-2 marks oocyte proteins for degradation in response to meiotic maturation. Curr. Biol. *16*, 56–62.

Sun, Y., Goderie, S.K., and Temple, S. (2005). Asymmetric distribution of EGFR receptor during mitosis generates diverse CNS progenitor cells. Neuron *45*, 873–886.

Tejedor, F., Zhu, X.R., Kaltenbach, E., Ackermann, A., Baumann, A., Canal, I., Heisenberg, M., Fischbach, K.F., and Pongs, O. (1995). minibrain: a new

protein kinase family involved in postembryonic neurogenesis in Drosophila. Neuron *14*, 287–301.

Yabut, O., Domogauer, J., and D'Arcangelo, G. (2010). Dyrk1A overexpression inhibits proliferation and induces premature neuronal differentiation of neural progenitor cells. J. Neurosci. *30*, 4004–4014.

Zhang, R., Zhang, Z., Zhang, C., Zhang, L., Robin, A., Wang, Y., Lu, M., and Chopp, M. (2004). Stroke transiently increases subventricular zone cell division from asymmetric to symmetric and increases neuronal differentiation in the adult rat. J. Neurosci. *24*, 5810–5815.

Zhao, C., Deng, W., and Gage, F.H. (2008). Mechanisms and functional implications of adult neurogenesis. Cell *132*, 645–660.

Zhong, W., and Chia, W. (2008). Neurogenesis and asymmetric cell division. Curr. Opin. Neurobiol. *18*, 4–11.